Supporting Information

Voltage-Induced Fluorescence Lifetime Imaging of a BODIPY Derivative in Giant Unilamellar Vesicles (GUVs) as Potential Neuron Membrane Mimics

Dumitru Sirbu, Lingli Zeng, Paul G. Waddell, Nikolai V. Tkachenko, Stanley W. Botchway, Andrew C. Benniston

Table of Contents

Experimental Details

Materials and Instrumentation

All NMR data processing were carried out with MestReNova software (version 11.0.0, Mestrelab Research S.L., A Coruña, Spain). Chemical shifts for ^{1}H-NMR, ^{13}C-NMR were reported relative to residual protiated solvent acetonitrile-d_3 (Cambridge Isotope Laboratories, Inc., CD_3CN, 99.8%) at δ = 1.940 ppm, quintet. The chemical shifts for ^{11}B-NMR are referenced relative to $BF_3 \cdot Et_2O$ at $\delta = 0$ and ^{19}F-NMR chemical shifts are referenced to $CFCl_3$ at $\delta = 0$ as external reference. Coupling constants (J) are given in Hz. Multiplicities of signals are indicated by the following abbreviations: s (singlet), d (doublet), t (triplet), q (quartet), dd (doublet of doublets), m (multiplet) and b (broad). High resolution mass spectra were measured using an Agilent 6550 i-Funnel system. Chromatography experiments were performed on Agilent 1260 Infinity HPLC system equipped with Raptor C18 column (100 × 3 mm; 2.7 μm particle size) using water/acetonitrile 1/9 mixture as eluent (0.3 mL min^{-1}) and compared to the solvent blank run. Diode Array Detector (1260 DAD VL+) was fixed in the spectral region of interest at 630 nm. UV-visible absorption spectra were performed on a Shimadzu Spectrophotometer UV-1800 (Shimadzu Corporation, Japan) reference cell and the other as a sample cell in the dual-beam UV-Vis system. 2D and 3D fluorescence excitation/emission spectra were obtained from a Shimadzu RF-6000 Fluorescence Spectrometer (Shimadzu Corporation, Japan), which was equipped with a 150 Watt Xenon lamp and controlled by LabSolutions RF software (Shimadzu Corporation, Japan). Peak deconvolution to Gaussian bands was performed using PeakFit™ program (version. 4.12, Systat Software, Inc., U.S.).

X-Ray Crystallography

All crystallography measurements were performed using in-house facilities at Newcastle University. Crystal structure data which were collected in-house used an Xcalibur, Atlas, Gemini ultra-diffractometer equipped with a sealed X-ray tube (λ CuKα = 1.54184Å) and a CryostreamPlus open-flow N_2 cooling system (Oxford Cryosystems Ltd, UK). Software CrysAlisPro (Version 1.171.37.35, Agilent Technologies, U.S.) was used for cell refinement, data collection, data reduction and intensities correction for absorption.

Synthesis

Preparation of BD

BD was synthesised by a modified reported literature method.[1] Pyrrole-2-carboxaldehyde (770.3 mg, 8.1 mmol, 1 e.q.) was dissolved in dry DCM (39 mL) and cooled down to -3 °C under a nitrogen atmosphere. 3-ethyl-2,4-dimethyl-1H-pyrrole (1.1 mL, 8.1 mmol, 1 e.q.) was added to the reaction mixture which was stirred for 10 mins, followed by slow addition of $POCl_3$ (0.76 mL, 8.1 mmol, 1 e.q.). The reaction mixture was stirred for 3h during which time the temperature was left to rise from -3 °C to R.T. The reaction mixture turned from pale orange to dark orange. Once the starting materials were consumed as followed by TLC, Et_3N (6.7 mL, 48.6 mmol, 6 e.q.) and after 5 mins $BF_3.OEt_2$ (6 mL, 48.6 mmol, 6 e.q.) were added sequentially to an ice-cold reaction mixture. The resulting solution was stirred for 1.5 h as the solution was left to equilibrate from 0 °C to R.T. The reaction mixture became dark brown. The reaction was washed three times with sat. $NaHCO_3$ and H_2O (50 mL) sequentially. The separated organic layer was concentrated and passed through a silica plug using pure DCM to remove most of the impurities. The crude product was further purified by silica gel column chromatography (eluent: DCM: petroleum ether, 20-60%, v/v) to afford the final product **BD** as a pale yellow solid with a strong green fluorescence. (1.1 g, 4.4 mmol, 55% yield); ^{1}H NMR (300 MHz, Chloroform-*d*) δ (ppm) = 7.60 (d, 1H), 7.15 (s, 1H), 6.89 (d, J = 2.8 Hz, 1H), 6.42 (dd, J_1 = 3.9 Hz, J_2 = 2.1 Hz, 1H), 2.60 (s, 3H), 2.43 (q, J = 7.6 Hz, 2H), 2.21 (s, 3H), 1.11 (t, J = 7.6 Hz, 3H). ^{13}C NMR (75 MHz, Chloroform-*d*) δ (ppm) = 163.44, 141.18, 137.98, 136.32, 134.91, 132.40, 125.36, 123.62, 115.70, 17.39, 14.34, 13.43, 9.59. ^{11}B NMR (96 MHz, Chloroform-*d*) δ (ppm) = 0.60 (t, J = 30.9 Hz). ^{19}F NMR (282 MHz, Chloroform-*d*) δ (ppm) = -146.06 (q, J = 31.2 Hz). HRMS (m/z): found $[M - F]^+$: 229.1340, calcd for $C_{13}H_{15}BFN_2$: 229.1315

Preparation of aJBD

JUL-CHO (92.6 mg, 0.46 mmol, 1.1 e.q.), piperidine (0.415 mL, 4.2 mmol, 10 e.q.) and glacial acetic acid (0.24 mL, 4.2 mmol, 10 e.q.) were added to a solution of **BD** (104 mg, 0.42 mmol, 1 e.q.) in anhydrous CH_3CN (17 mL) containing 4Å dry molecular sieves (1 g). The resulting mixture was refluxed under nitrogen for 2.5 hours and monitored by TLC until the complete consumption of the starting material. The colour changed from dark brown to dark blue. The molecular sieves were removed by a sinter funnel and washed with DCM till

colourless. All the collected DCM and original CH_3CN solutions were removed by a rotary evaporator. The crude product was redissolved in Et_2O: hexane (1:1) and purified by preparative alumina TLC (eluent: Et_2O: hexane, 1:1) to give the pure product **aJBD** as a black solid with a metallic green colour. (58 mg, 0.13 mmol, 32% yield); ^{1}H NMR (400 MHz, Chloroform-*d*) δ (ppm) = 7.56 (m, 1H), 7.43 (apparent tr, *J* = 17 Hz 2H, *trans* CH=CH), 7.10 (s, 2H, -CH-phenylJUL), 6.98 (s, 1H), 6.77 (d, *J* = 2.8 Hz, 1H), 6.38 (dd, J_1 = 3.8 Hz, J_2 = 2.1 Hz, 1H), 3.26 (t, *J* = 5.8 Hz, 4H, -CH_2-JUL), 2.76 (t, *J* = 5.8 Hz, 4H, -CH_2-JUL), 2.68 (q, *J* = 7.5 Hz, 2H), 2.18 (s, 3H), 1.97 (m, 4H, -CH_2-JUL), 1.22 (t, *J* = 7.5 Hz, 3H). ^{13}C NMR (101 MHz, Chloroform-*d*) δ (ppm) = 158.78, 145.08, 142.09, 140.85, 137.93, 135.74, 135.08, 132.81, 127.69, 123.73, 122.60, 121.33, 119.35, 115.05, 113.18, 50.15, 27.80, 21.73, 19.10, 13.79, 9.27. ^{11}B NMR (96 MHz, Chloroform-*d*) δ (ppm) = 1.03 (t, *J* = 32.6 Hz). ^{19}F NMR (282 MHz, Chloroform-*d*) δ (ppm) = -143.00 (q, *J* = 32.1 Hz). The measured molar extinction coefficient at 648 nm for **aJBD** in DMSO is 58,000 M^{-1} cm^{-1}. HRMS (m/z): found $[M + H]^+$: 432.2446, calcd for $C_{26}H_{29}BF_2N_3$: 432.2427; HPLC (min): 8.877.

Quantum Yield and Solution Fluorescence Lifetime Measurements

For fluorescence quantum yields (Φ_{FLU}) measurements in different solutions, were measured using the relative quantum yield method with respect to the reference dye Cy643. All the samples and the reference were prepared freshly in appropriate solvents on the day of use. The optical density (OD) of the UV absorbance was less than 0.05 at the excitation wavelength. Fluorescence areas were calculated by the instrument software (LabSolutions RF software) using the corresponding fluorescence spectra. Quantum yields were corrected for changes in refractive index of the solvents. Solution fluorescence lifetime measurements for **aJBD** were recorded by an upright confocal microscope which comprised of a SPC-150 TCSPC module (Becker & Hickl, Berlin, Germany).

Time Resolved Transient Absorption Spectroscopy

Excited state dynamic processes of **aJBD** in femtosecond to nanosecond time scales were performed by transient absorption spectroscopy. A 590 nm pump pulse (100 fs fwhm) was applied to excite the **aJBD** complex. The sample solution was prepared in two different solvents (hexane and DMSO) with an optical density between 0.2-0.8 in a 2 mm cuvette. The data were globally fitted to get the relaxation time constants and the associated decay component spectra. Also, steady-state absorption spectra were measured before and after the

pump-probe measurement to make sure that the sample did not change during the measurement.

Preparation of Giant Unilamellar Vesicles (GUVs)

GUVs were prepared by the electroformation method. The whole apparatus for preparing GUVs was precleaned with EtOH in a bath sonicator for 30 min, and dried under nitrogen carefully to remove all the house dust which would impact on the GUVs growing. The test chamber was assembled with one piece of coverslip at the bottom with two platinum wires suspended on it. The lipid solution of 1-palmitoyl-2-oleoyl-sn-glycero-3-phosphocholine (POPC) was prepared in a $CHCl_3$: MeOH (2: 1, v/v) mixture. An appropriate mixture of POPC lipid (4 μL on each wire) was deposited onto two parallel platinum wires respectively, and the solvent was evaporated for 30 mins till completely dry. Sucrose solution (300 mM, 2 mL) was added into the assembled chamber. The chamber was subjected to an alternating current (AC) frequency of 10 Hz with an output voltage of 3.3 Vpp at 50 °C for 1.5 hours. GUVs were stained with **aJBD** (2 μL, 50 μM) in the testing chamber prior to the microscopy measurements.

GUVs Fluorescence Lifetime Imaging

The presence of GUVs in solutions were firstly checked by confocal microscopy, and FLIM measurements were performed on a modified Nikon Eclipse Ti-U inverted microscope (Nikon Instruments Inc., Melville, NY, USA) at the Rutherford Appleton Laboratory. Laser light was focused through a 60 x water immersion plan-apochromat objective with a numerical aperture of 1.2. The GUVs were imaged while samples were excited at 633 nm with an acousto-optic tuneable filters (AOTF) coupled with a fianium supercontinuum light source (Fianium, NKT Photonics, Southampton, UK), which was tuneable (400-2000 nm) and produced 40 ps laser pulses at 40 MHz (25 ns between laser pulses). In the one-photon laser scanning, 256 × 256 pixels/decay curves were used. Fluorescence lifetime images were obtained using the SPCImage analysis software (version 9.80, Becker & Hickl GmbH, Germany) using the SPC-150 mode. The decay trace for each pixel with a pixel bin of 10 was best fit to a single or double exponential model to allow analysis in the nanosecond decay domain. The quality of a goodness-of-fit was judged by the chi-squared value (χ^2).

For the ramping voltage experiment, the applied voltage was gradually increased from 0 mV to 100 mV, 200 mV, 300 mV then back to 0 mV followed by lifetime measurements at the same time. Each fluorescence lifetime image was collected for 20 sec. For the ON-OFF cycles GUVs were depolarized for 5 seconds with 250 mVpp voltage. A GUV was subjected to "on-off" direct current (DC) pulse for 50 "on-off" cycles after depolarization. Each cycle included 20 seconds with voltage applied (600 mVpp) which was called "on" and 20 seconds for the resting state (0 mVpp) which was called "off". A fluorescence lifetime image was collected for 20 seconds during each "on" or "off" process.

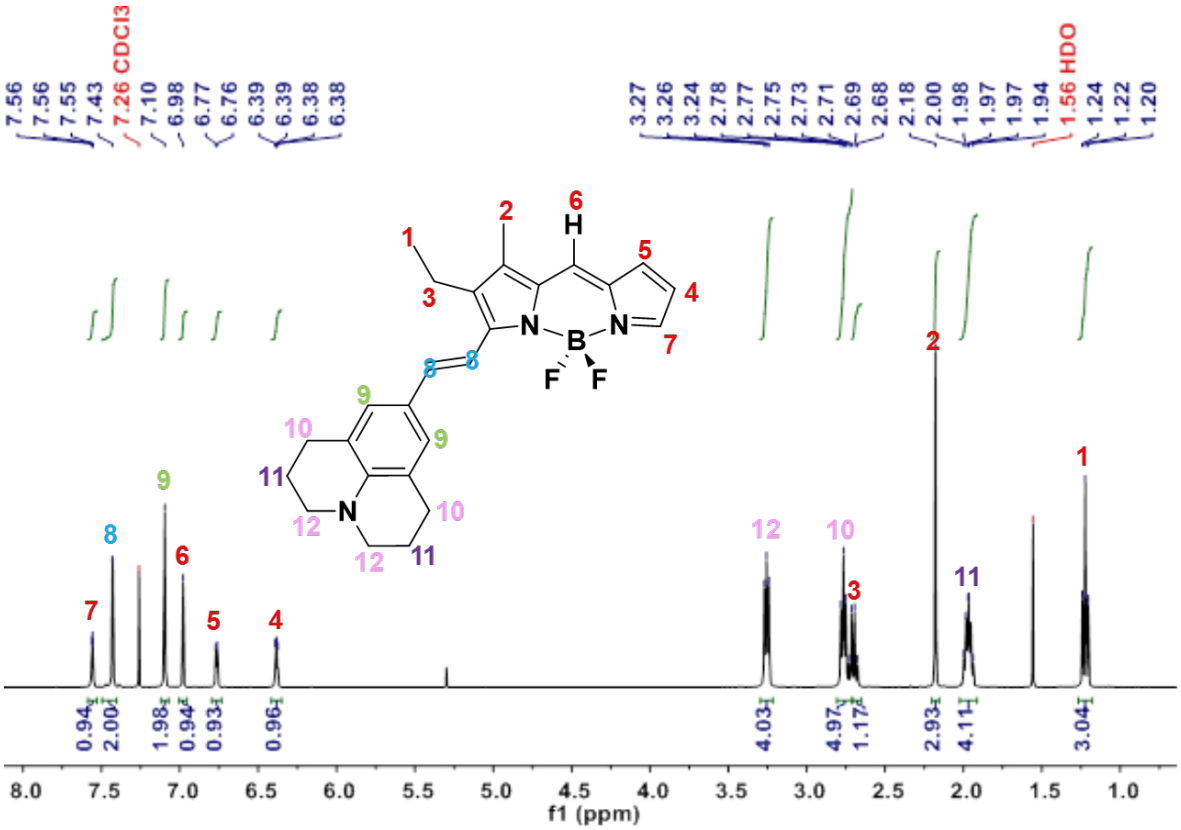

Figure S2. ^{1}H NMR spectrum recorded at R.T. of **aJBD** in $CDCl_3$.

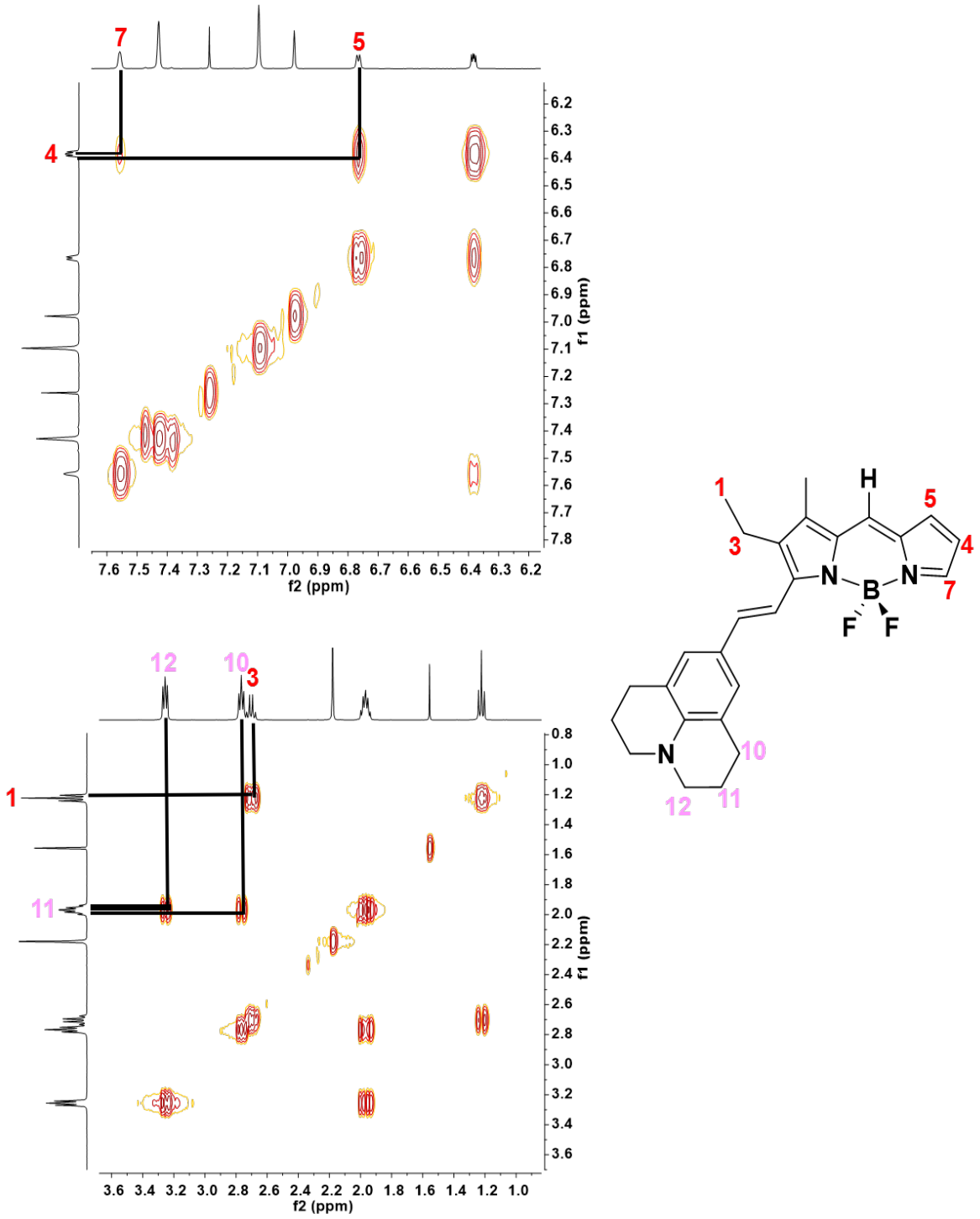

Figure S3. COSY spectra recorded at R.T. of **aJBD** in $CDCl_3$.

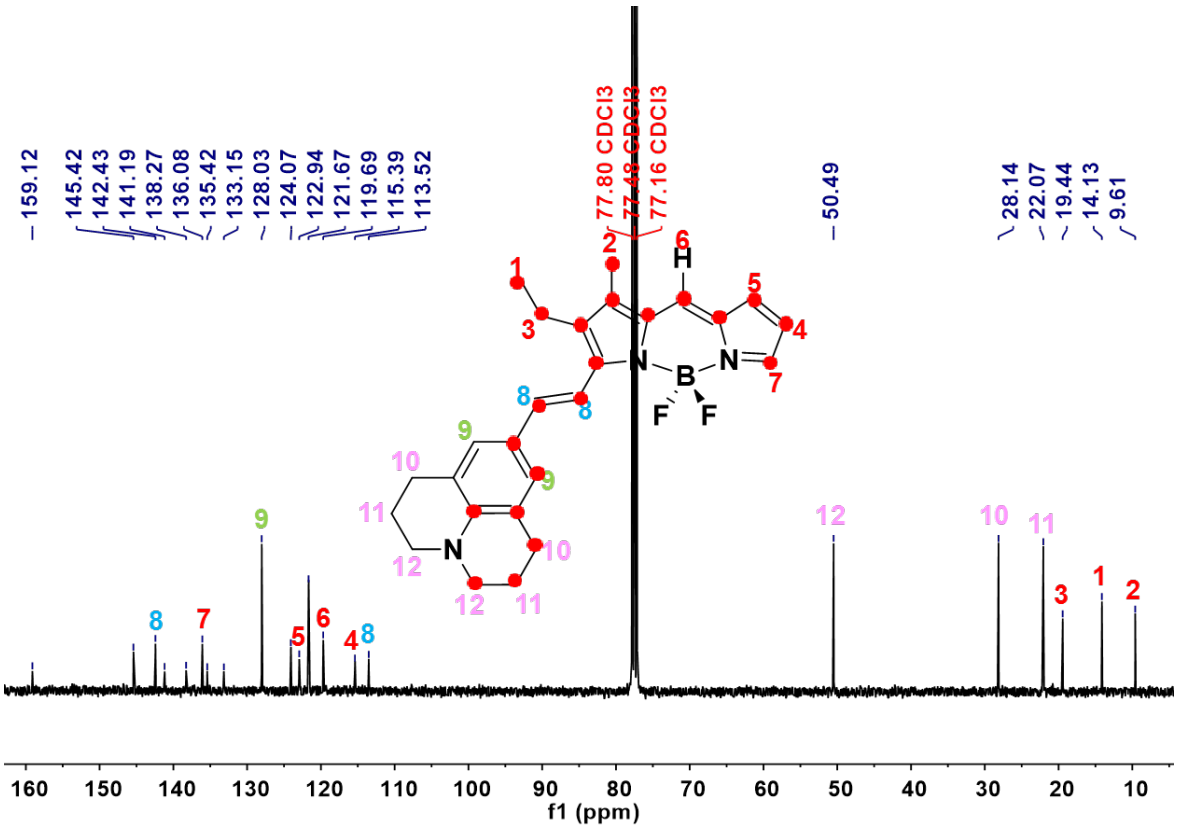

Figure S4. ^{13}C NMR spectrum recorded at R.T. of **aJBD** in $CDCl_3$.

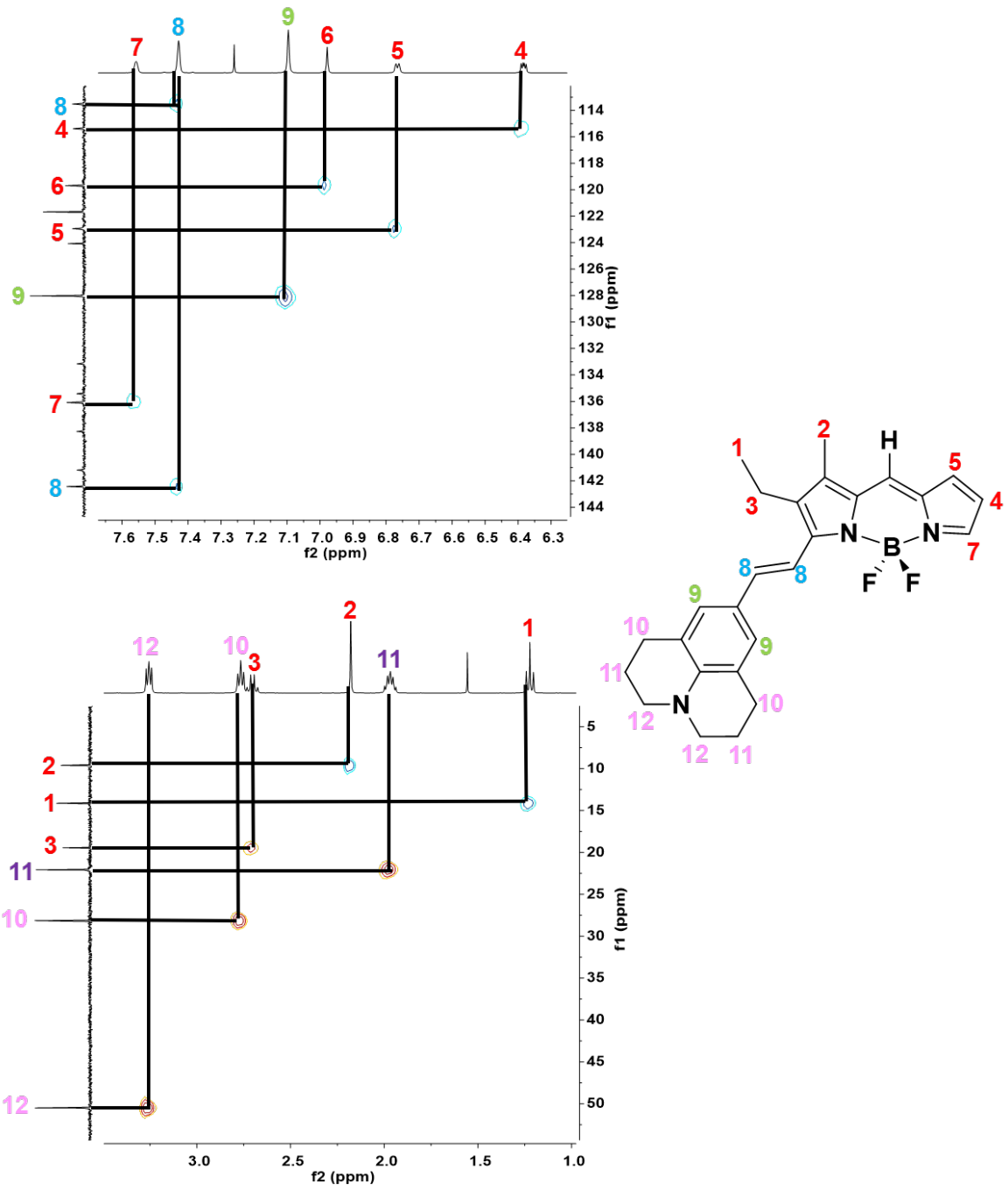

Figure S5. HSQC spectra recorded at R.T. of **aJBD** in $CDCl_3$ showing proton-to-carbon correlations and their assignments.

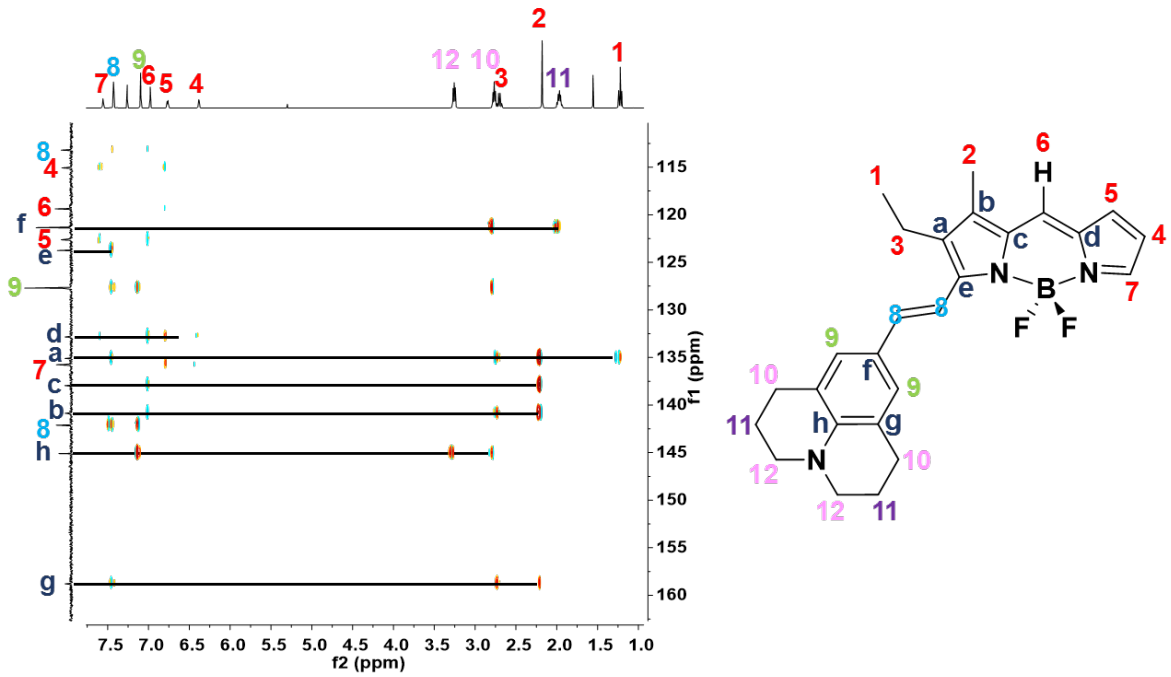

Figure S6. HMBC spectrum recorded at R.T. of **aJBD** in $CDCl_3$ showing proton-to-carbon correlations and their assignments.

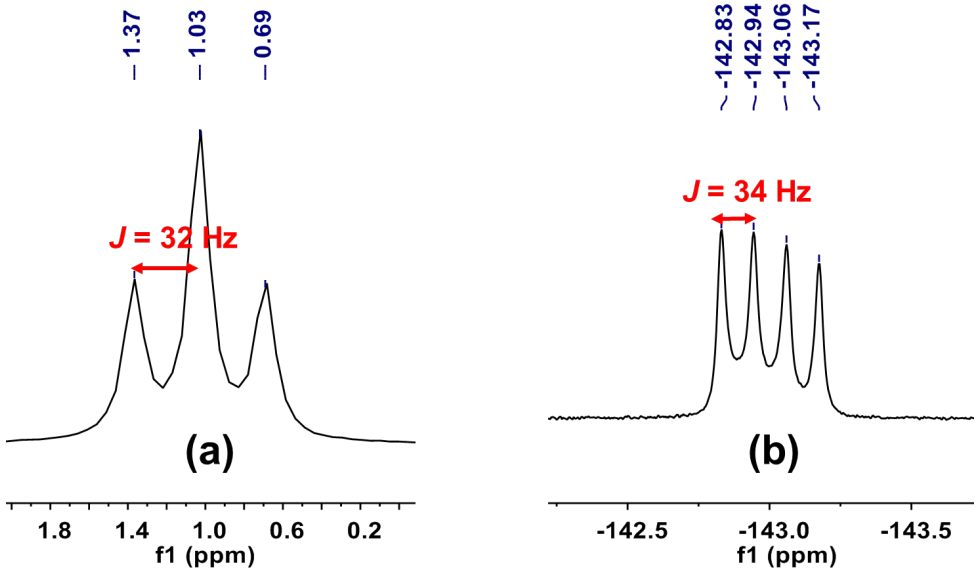

Figure S7. ^{11}B **(a)** and ^{19}F **(b)** NMR spectra recorded at R.T. of **aJBD** in $CDCl_3$.

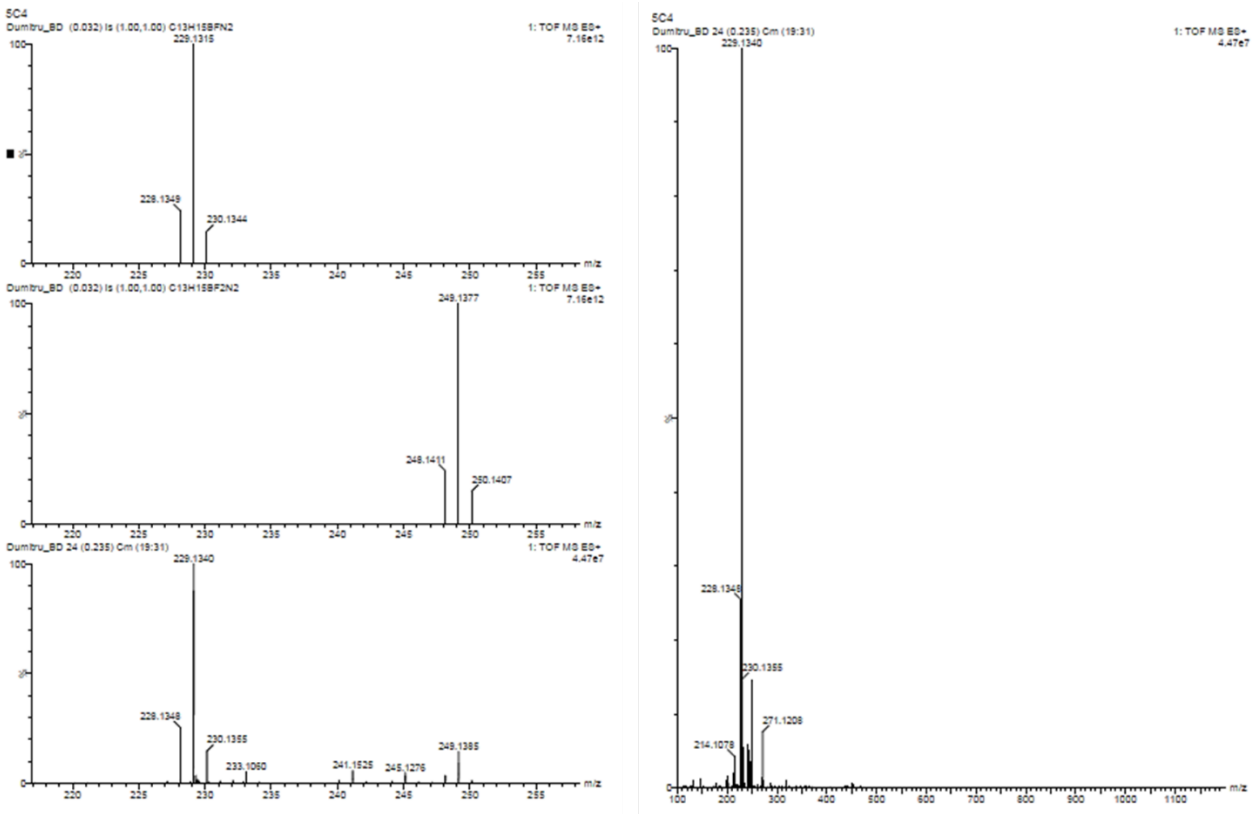

Figure S7. Left: Observed (bottom) and theoretical mass spectra for $[M\text{-}F]^+$ (top) and $[M+H]^+$ (middle) cations for **BD**. Right: Full observed mass spectrum of **BD**.

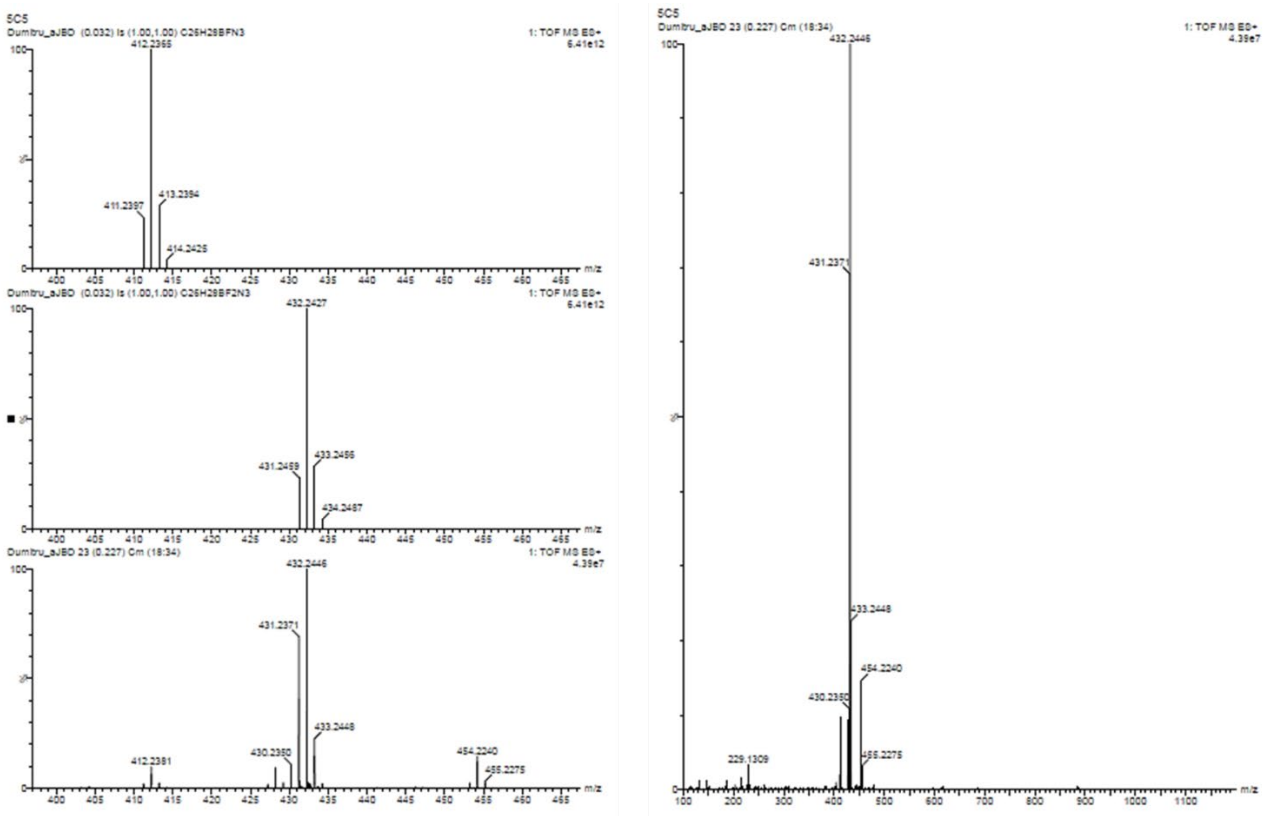

Figure S8. Left: Observed (bottom) and theoretical mass spectra for $[M\text{-}F]^+$ (top) and $[M+H]^+$ (middle) cations for **aJBD**. Note: the m/z 454 peak corresponds to the $[M+Na]^+$ adduct. Right : Full observed mass spectrum of **aJBD**.

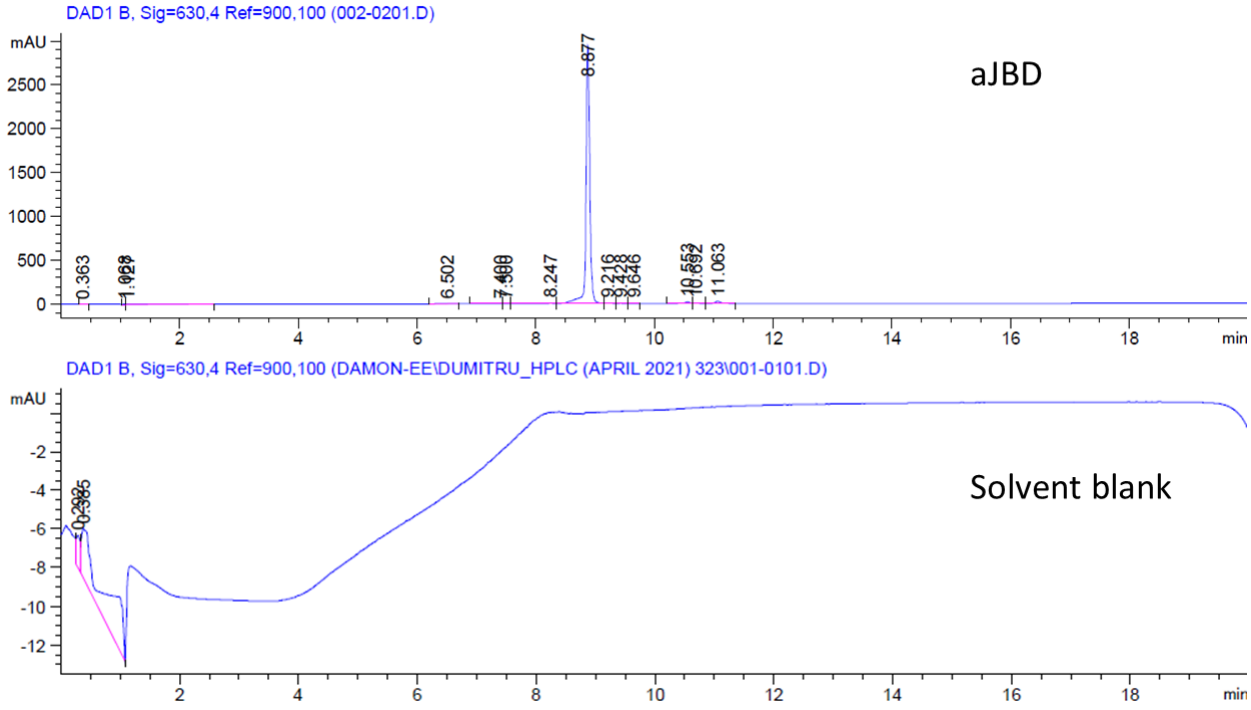

Figure S9. Isocratic HPLC trace for **aJBD** and the solvent blank. Solvent = MeCN/H_2O.

Table S1. Crystal data and structure refinement for **aJBD**

Identification code	acb160009_sa
Empirical formula	$C_{27}H_{30}BCl_2F_2N_3$
Formula weight	516.25
Temperature/K	150.0(2)
Crystal system	triclinic
Space group	P-1
a/Å	11.0740(7)
b/Å	11.1150(6)
c/Å	12.1059(9)
α/°	85.621(5)
β/°	75.257(6)
γ/°	61.941(6)
Volume/Å^3	1270.01(16)
Z	2
ρ_{calc}g/cm^3	1.350
μ/mm^{-1}	2.596
F(000)	540.0
Crystal size/mm^3	0.48 × 0.18 × 0.05
Radiation	CuKα (λ = 1.54184)
2Θ range for data collection/°	7.562 to 133.872
Index ranges	-13 ⩽ h ⩽ 12, -13 ⩽ k ⩽ 12, -14 ⩽ l ⩽ 14
Reflections collected	18190
Independent reflections	4498 [R_{int} = 0.0547, R_{sigma} = 0.0499]
Data/restraints/parameters	4498/0/318
Goodness-of-fit on F^2	1.038
Final R indexes [I>=2σ (I)]	R_1 = 0.0497, wR_2 = 0.1095
Final R indexes [all data]	R_1 = 0.0712, wR_2 = 0.1251
Largest diff. peak/hole/e Å^{-3}	0.79/-0.63

(a) **(b)**

Figure S10. (a) Stick-style structure of the julolidine head group with respect to the BODIPY core showing the out-of-plane nature of the molecule; **(b)** Perpendicular relationship between the plane of the two fluorine atoms and the plane of the BODIPY core.

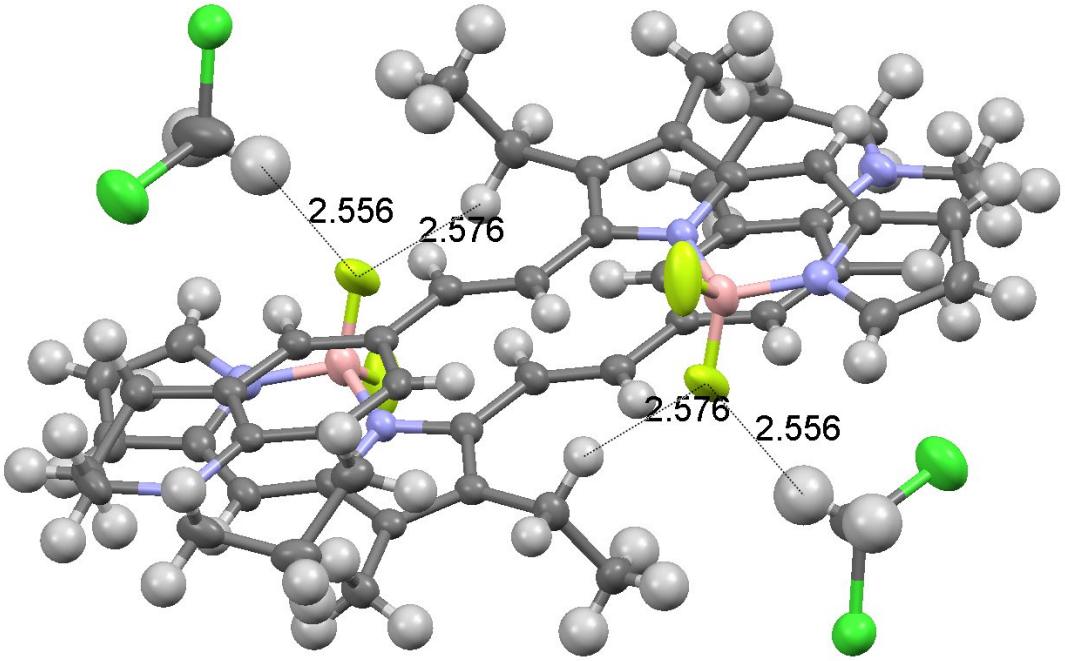

Figure S11. Crystal packing diagram showing H—F distances between the methylene proton of the ethyl unit and methylene proton of the CH_2Cl_2 solvate with the BF_2 group.

Table S2. Selected average bond lengths and bond angles for **aJBD**.

Atoms	**Bond Length/Å**	
C14-C15	1.347 (4)	Trans C=C
F1-B4	1.378 (4)	
F2-B4	1.393 (4)	
N1-B4	1.533 (4)	
N2-B4	1.553 (3)	
N3-C19	1.379 (3)	Julolidine
N3-C24	1.459 (4)	
N3-C27	1.457 (4)	
C16-C21	1.394 (4)	
C16-C17	1.407 (4)	
C21-C20	1.375 (3)	
C17-C18	1.388 (4)	
C25-C20	1.517 (4)	
C20-C19	1.414 (4)	
C19-C18	1.420 (4)	
C18-C22	1.498 (4)	
C25-C26	1.515 (4)	
C22-C23	1.521 (4)	
C26-C27	1.511 (4)	
C23-C24	1.515 (4)	
F1-B4-F2	109.2 (2)	
N1-B4-N2	107.7 (2)	
C2-C12-C13	114.1 (2)	
Atoms	**Dihedral Angle/°**	
C14-C15-C16-C17	2.91	JUL-BODIPY
C18-C22-C23-C24-N3	132.22	JUL-JUL
C20-C25-C26-C27-N3	135.22	JUL-JUL

Table S3. List of selected UV-Vis absorption and emission spectroscopic data for **aJBD** and quantum yield measurements in different solvents at R.T. Solvents are arranged in order of dielectric constants from top to bottom in sequence.

Solvent	λ_{ABS} [a]/nm	λ_{ABS} [a]/cm^{-1}	λ_{EM} [a]/nm	λ_{EM} [a]/cm^{-1}	Stokes' Shift/cm^{-1}	Φ_f [b] /%
Hexane	623.5	16038	644	15528	511	100
Cyclohexane	630	15873	648	15432	441	100
Toluene	636	15723	694.5	14399	1324	72
Oleic Acid	634	15773	675	14815	958	61
Linoleic Acid	634	15773	680.5	14695	1078	47
Diethyl Ether	622	16077	693.5	14420	1658	35
Chloroform	641	15601	718.5	13918	1683	17
THF	630	15873	727.5	13746	2127	2.6
Decanol	635.5	15736	701.5	14255	1480	13
Octanol	630.5	15860	705	14184	1676	10
Heptanol	632.5	15810	701.5	14255	1555	6.7
Hexanol	634	15773	710	14085	1688	4.6
1-Pentanol	629.5	15886	712	14045	1841	3.3
1-Butanol	630	15873	716	13966	1907	1.9
Cyclohexene	633.5	15785	684	14620	1165	30
Iso-Propanol	627.5	15936	719.5	13899	2038	1.2
Ethanol	627.5	15936	721.5	13860	2076	0.5
Methanol	626	15974	664	15060	914	0.2
DMF	637.5	15686	648	15432	254	0.8
DMSO	649	15408	*na*	*na*	*na*	<0.1

[a] Absorption and emission (λ_{ex} = 590 nm) maxima data obtained from experimental measurements from the instruments. [b] Data are the quantum yields measured relative to **Cy643** in MeOH. (Φ_{Cy643} = 43%). To convert wavelength to wavenumber, the following formula was used: $\tilde{\nu} = 1/\lambda$; $\tilde{\nu}$ is wavenumber (cm^{-1}) and λ is wavelength (nm). The Stokes' shift (SS) was calculated by $\lambda_{abs} - \lambda_{em}$ in wavenumbers (cm^{-1}).

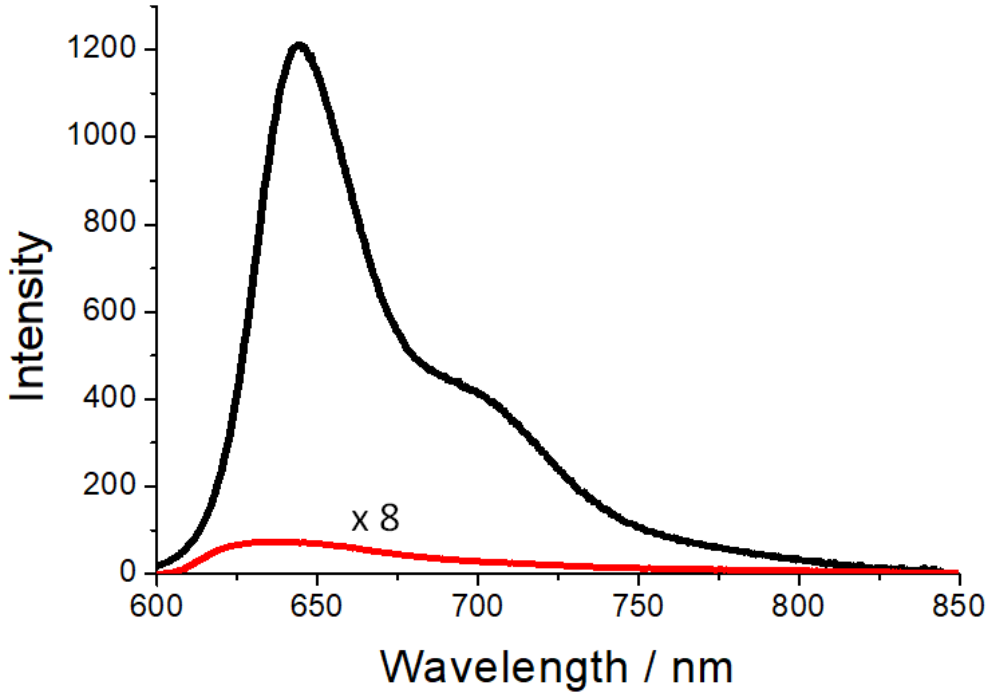

Figure S12. Room temperature fluorescence spectra of **aJBD** in hexane (black) and DMF (red).

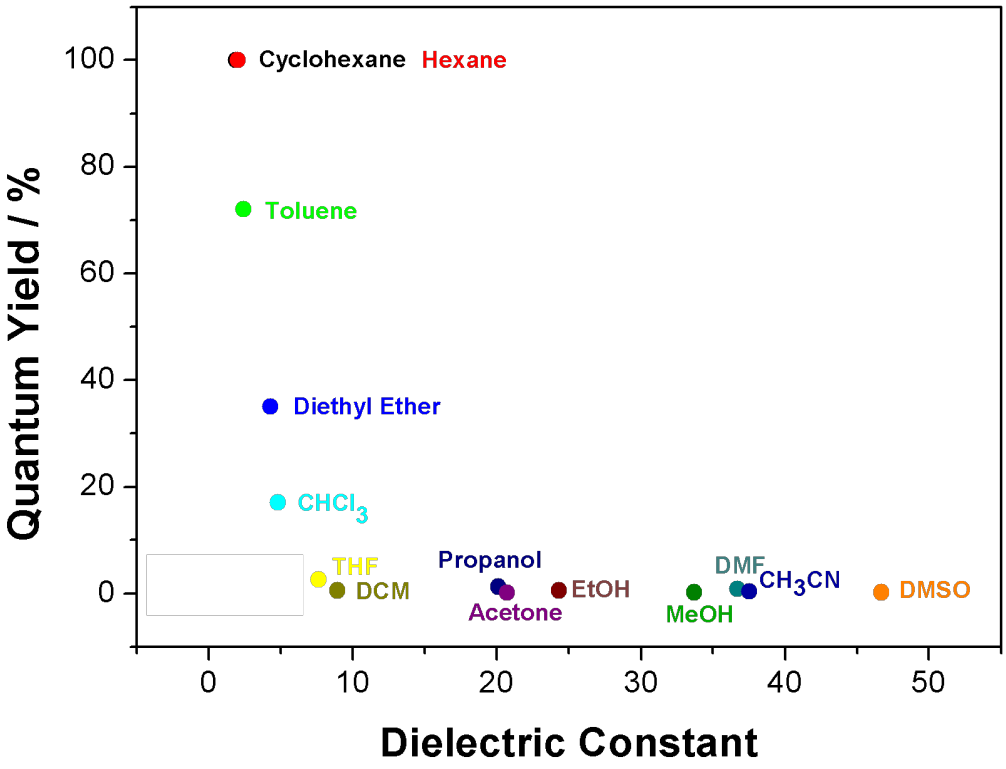

Figure S13. Relationship between fluorescence quantum yield and dielectric constant for **aJBD** in various solvents.

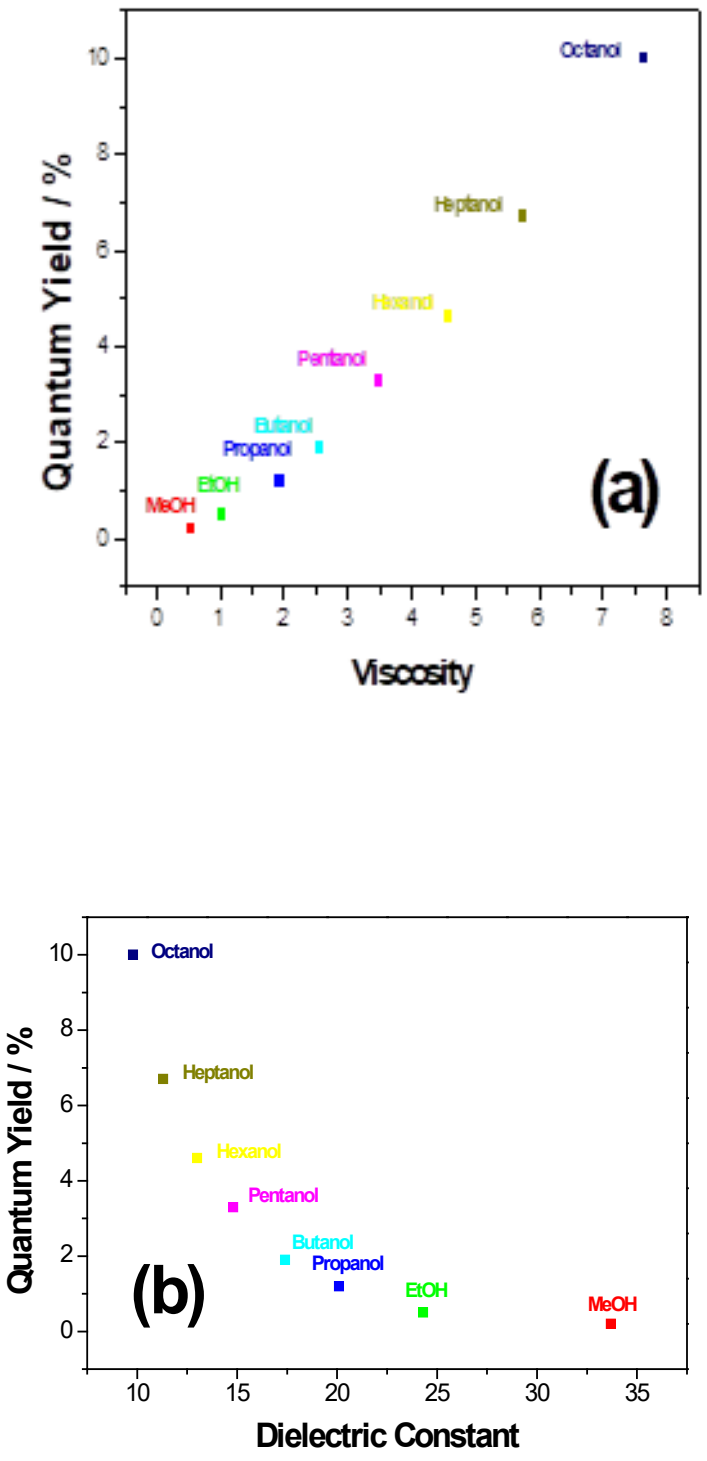

Figure S14. (a) Plot of fluorescence quantum yields to solvent viscosity for the linear mono-protic alkanol solvents. **(b)** Plot of fluorescence quantum yields to solvent dielectric constant for the linear mono-protic alkanol solvents.

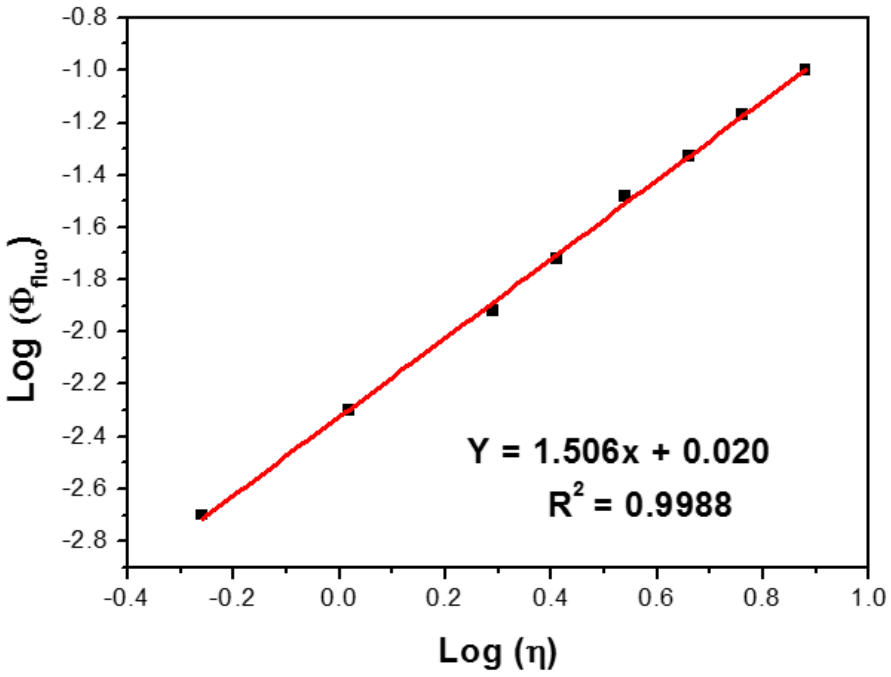

Figure S15. Fluorescence quantum yield and viscosity relationship and the fitting of the data to the Förster-Hoffmann Equation for linear mono-protic alkanols.

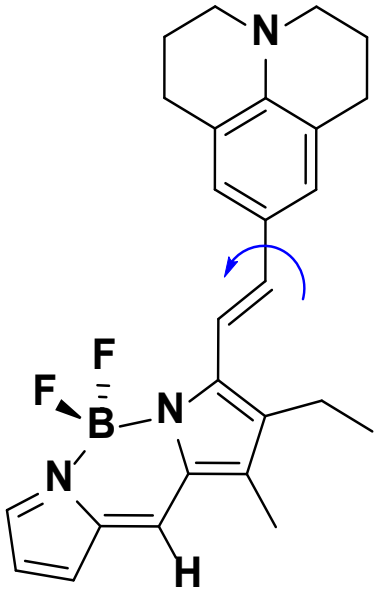

Figure S16. Possible rotation between the julolidine and BODIPY units.

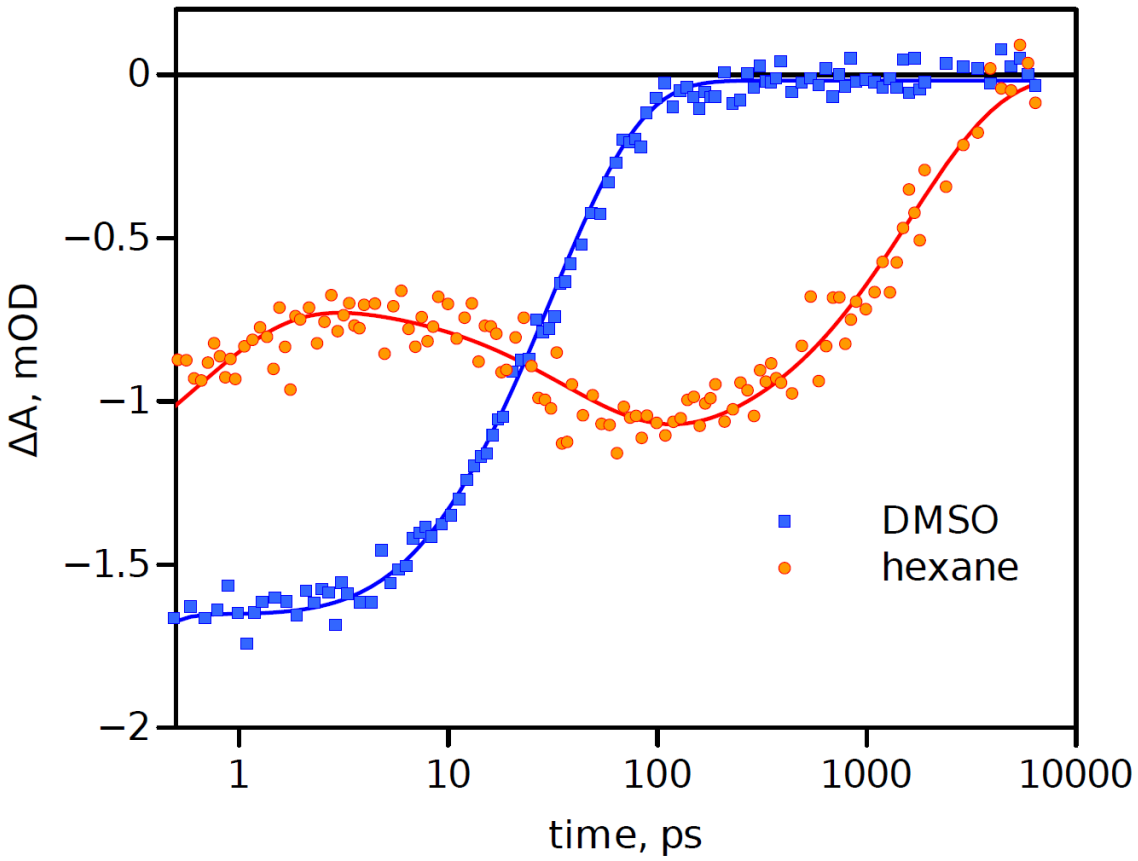

Figure S17. Time profile for **aJBD** recorded at 640 nm from pump-probe experiments in DMSO and hexane.

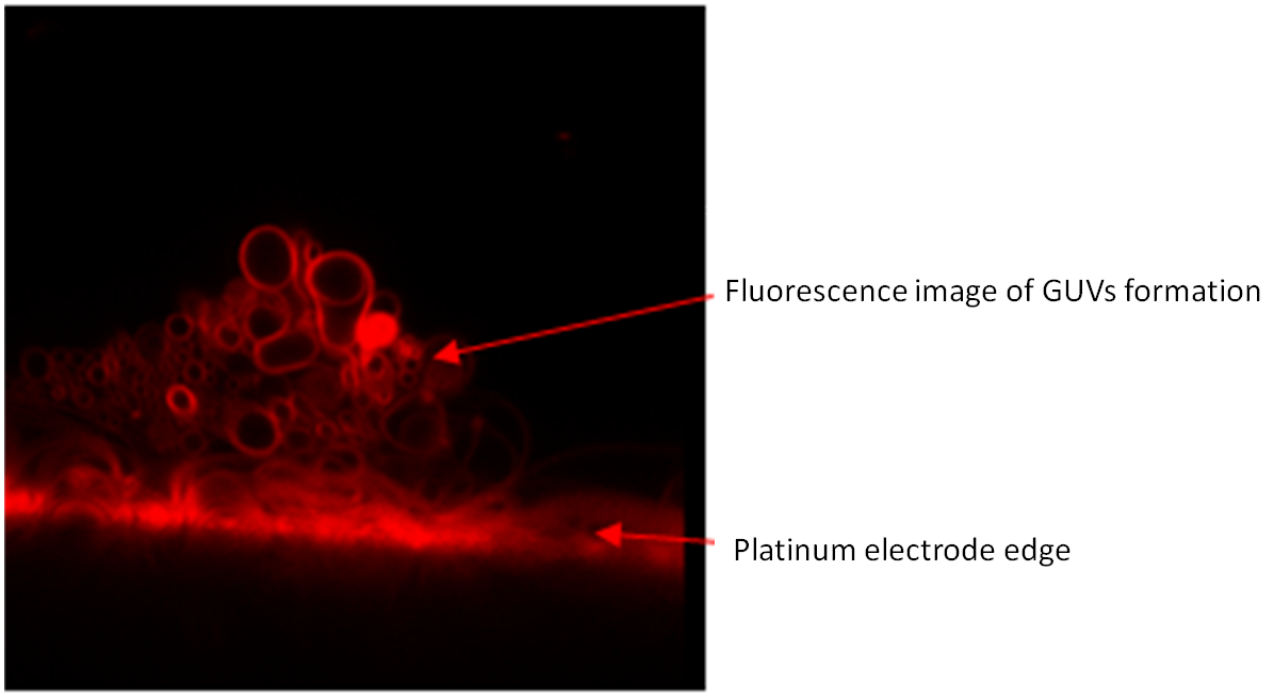

Figure S18. Fluorescence image of GUVs electroformation on a platinum electrode with **aJBD** stained in a 1-palmitoyl-2-oleoyl-sn-glycero-3-phosphocholine (POPC) sucrose solution.

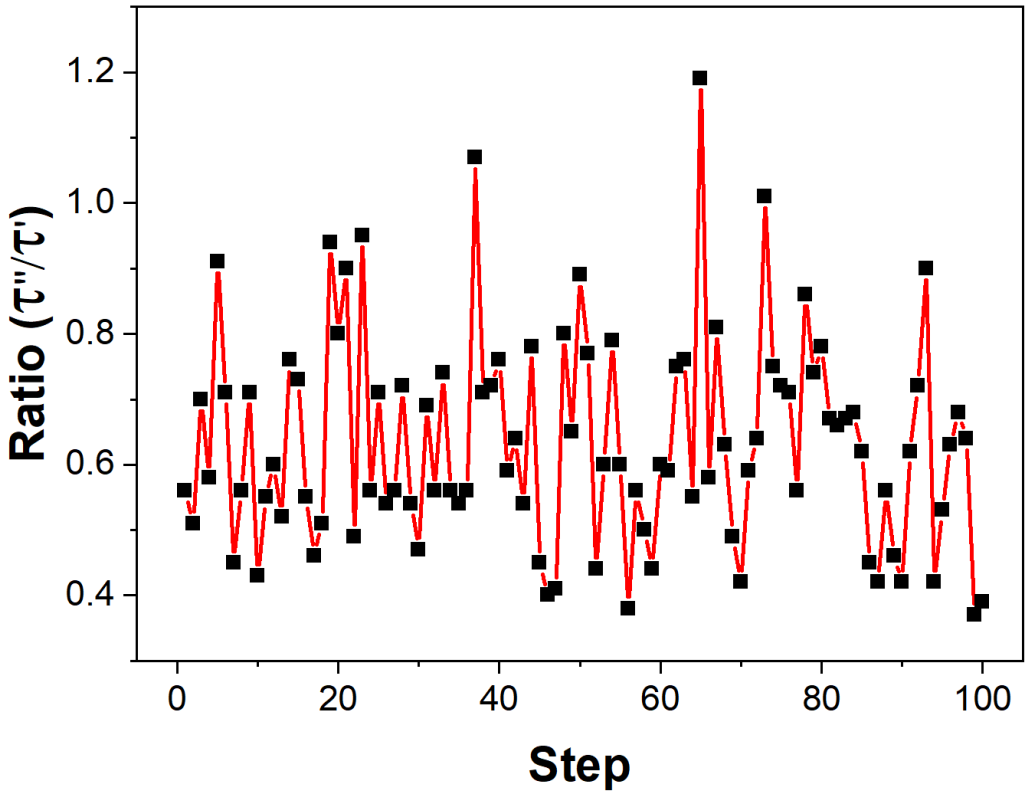

Figure S19. Distribution ratio plot of τ_1 versus τ_2 from τ_1 as collected over 50 ON-OFF cycles.

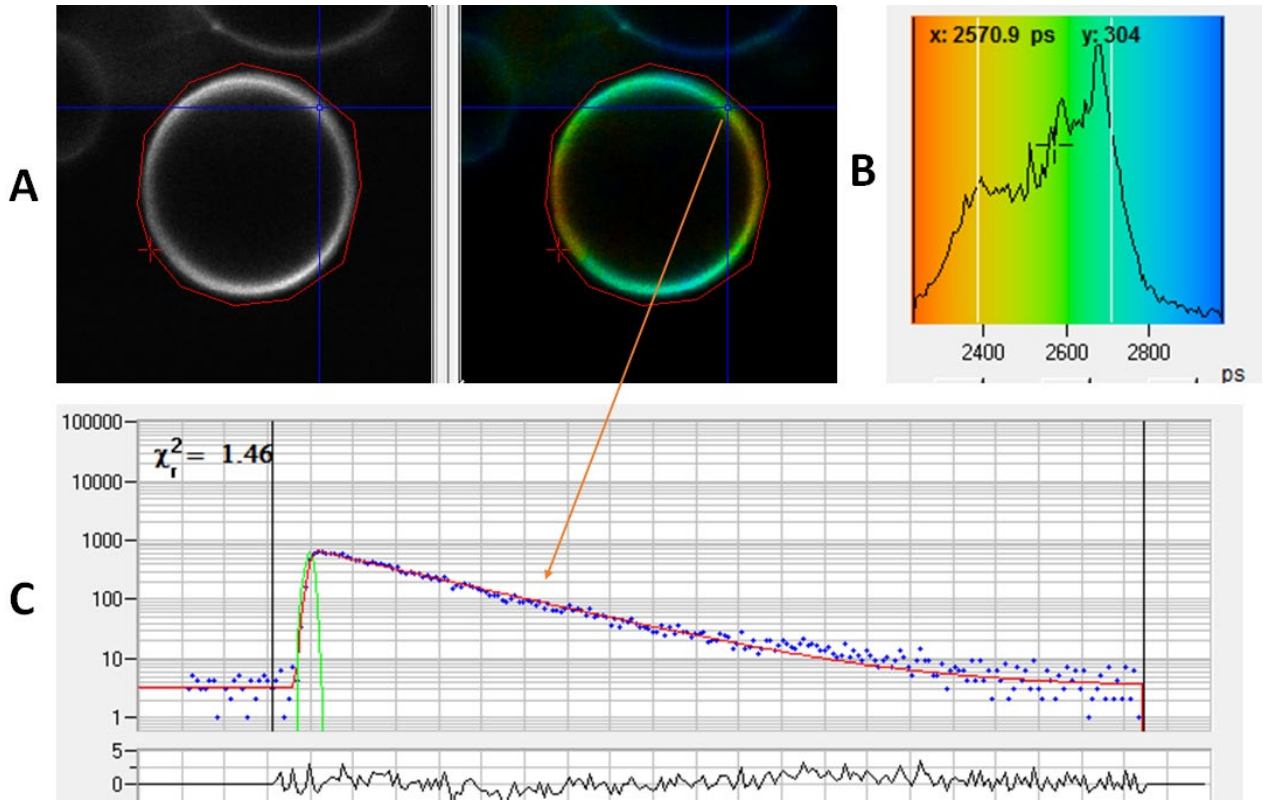

Figure S20. A GUV stained with the VSD dye Di-4-ANEPPS and the FLIM image (**A**) and the lifetime map (**B**) and decay profile (**C**).

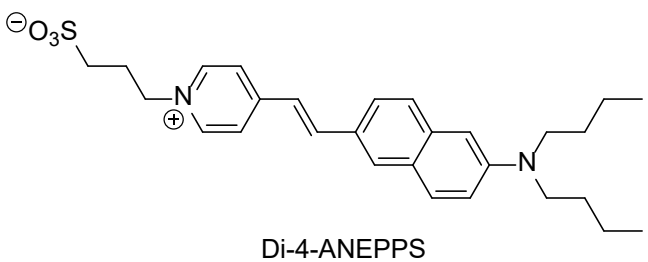

Di-4-ANEPPS

References

1. X. Zhou, C. Yu, Z. Feng, Y. Yu, J. Wang, E. Hao, Y. Wei, X. Mu and L. Jiao, *Org. Lett.*, 2015, **17**, 4632-4635.